PUBLICATIONS OF THE ASTRONOMICAL SOCIETY OF THE PACIFIC, **117**:000–000, 2005 January

MS# 205005 PASP 117(827) Copyeditor: jxe
Monday Dec 13 2004 03:25 PM

A CCD *BVI* Photometric Study of the Young, Highly Reddened Open Cluster NGC 6318

ANDRÉS E. PIATTI

Instituto de Astronomía y Física del Espacio, Casilla de Correos 67, Succursale 28, 1428 Buenos Aires, Argentina; andres@iafe.uba.ar

AND

JUAN J. CLARIÁ AND ANDREA V. AHUMADA

Observatorio Astronómico, Universidad Nacional de Córdoba, Laprida 854, 5000 Córdoba, Argentina; claria@mail.oac.uncor.edu, andrea@mail.oac.uncor.edu

Received 2004 November 5; accepted 2004 November 18; published 2004 December XX

ABSTRACT. We present CCD *BVI* photometry for the southern open cluster NGC 6318. The sample consists of 9876 stars measured in an area of 13′.6 × 13′.6, extending down to $V \sim 21.5$ mag. Star counts carried out within and outside the cluster region allowed us to estimate the cluster angular radius as ∼8′. The comparison of the cluster color-magnitude diagrams with isochrones of the Geneva group yields $E(B-V) = 1.20 \pm 0.05$, $E(V-I) = 1.55 \pm 0.10$, and $V - M_V = 15.45 \pm 0.35$ for $\log t = 8.20$ ($t = 160$ Myr) and $Z = 0.020$. NGC 6318 is then located at 2.1 ± 0.5 kpc from the Sun and 30 pc below the Galactic plane. Using the WEBDA open cluster database, we examined the structure of the Galactic disk along the line of sight of NGC 6318. Among the known clusters in this direction, HM 1 and BH 222 are the farthest ones, while those located between 1 and 2 kpc of the Sun appear to be more absorbed than those expected to follow a quasi-linear extinction law.

1. INTRODUCTION

The photometric data reported in this paper emerge from an observing project that is still being developed at the Observatorio Astronómico of the National University of Córdoba (Argentina). The main aim of such a project is that of obtaining CCD photometric and/or spectroscopic data of southern open clusters not yet observed or with only incomplete observations. In some cases, *BVI* photometry proved to be a valuable tool for obtaining the fundamental parameters of star clusters, since information on cluster membership, distance, interstellar reddening, and age are obtained through the analysis of $(V, B-V)$ and $(V, V-I)$ color-magnitude diagrams (CMDs; see, e.g., Piatti et al. 2000b; Piatti & Clariá 2002). In other cases, CCD photometric data obtained with the Johnson *V* and Kron-Cousins *I* filters were supplemented with Washington photometric data to determine the cluster fundamental parameters and, mainly, to estimate cluster metal content (see, e.g., Piatti et al. 2003, 2004).

NGC 6318 (IAU designation C1714−394), also known as M166 (Melotte 1915), CR 325 (Collinder 1931), or ESO 333−SC1 (Lauberts 1982), is a small-sized open cluster situated near the Galactic anticenter direction at $\alpha = 7^{\rm h}16^{\rm m}11^{\rm s}$, $\delta = -39°25'30''$ (J2000.0), with Galactic coordinates $l = 347.^{\circ}90$ and $b = -0.^{\circ}69$, as consigned in the WEBDA open cluster catalog (Mermilliod 2004). Although BH 218 (van den Bergh & Hagen 1975), centered at $\alpha = 17^{\rm h}16^{\rm m}12^{\rm s}$, $\delta = -39°24'00''$ (J2000.0), is considered to be a different, somewhat larger cluster than NGC 6318 in the WEBDA open cluster database, both S. Gottlieb and J. Kay have independently noted that NGC 6318 and BH 218 are, in fact, the same cluster (Archinal & Hynes 2003). These authors describe NGC 6318 = BH 218 as a Trumpler (1930) class III1m system; i.e., a detached cluster with no central concentration and with most stars of nearly the same brightness. In a preliminary study, Piatti et al. (2000a, hereafter PBC) obtained CCD *BVI* images in a 4′ × 4′ field centered on NGC 6318 using the 24 inch (0.6 m) telescope of the University of Toronto Southern Observatory (Las Campanas Observatory, Chile). They measured *V* magnitudes and $B-V$ and $V-I$ colors for only 244 stars, extending down to $V \sim 19$ mag. From the analysis of their CMDs, they determined $E(B-V) = 1.25 \pm 0.05$, $E(V-I) = 1.55 \pm 0.05$, and $V - M_V = 15.5 \pm 0.5$ and estimated a cluster age between 5 and 50 Myr. In addition, from a flux-calibrated integrated spectrum of NGC 6318, they derived $E(B-V) = 1.20$ and a cluster age of between 3 and 30 Myr. The latter values, however, should be treated with caution, because of the relatively low signal-to-noise ratio of the integrated spectrum of NGC 6318.

In this work, we present new CCD photometric data of NGC 6318 obtained in a stellar field 12 times larger than that used by PBC. These data were obtained using a telescope with a mirror ∼50% larger in radius, hence the number of stars observed in the NGC 6318 field is ∼40 times greater. The *V* limit magnitude reached also surpasses by ∼2 mag that of these authors, and the quality of the CMDs is consequently higher. The present data are used to more precisely determine the cluster fundamental parameters.

In § 2 we describe the observational material and the data

reduction. In § 3 we present a detailed analysis of the photometric data. In particular, we examine the degree of contamination by field stars in the CMDs, and we discuss the nature of the broadness of the cluster main sequence. In § 4, through the fitting of theoretical isochrones of the Geneva group, we redetermine the cluster parameters of reddening, distance, and age and compare them with those derived by PBC. Using the WEBDA open cluster database (Mermilliod 2004), we also examine the structure of the Galactic disk along the line of sight of NGC 6318.

2. OBSERVATIONS AND REDUCTIONS

CCD images of the cluster field were obtained with the Johnson *B* and *V* and Kron-Cousins *I* filters using the 0.9 m telescope at the Cerro Tololo Inter-American Observatory (CTIO; Chile) on 1998 June 17–18. The telescope was equipped with the 2048 × 2048 pixel Tektronix 2K No. 3 CCD, and the seeing was typically 1″.2 during the observing night. The detector used has a pixel size of 24 μm, producing a scale on the chip of 0″.4 pixel^{-1} (focal ratio f/13.5) and a 13′.6 × 13′.6 field of view. The CCD was controlled by the CTIO ARCON 3.3 data acquisition system in the standard quad amplifier mode, operating at a mean measured gain (four chips) of 1.15 ± 0.04 e^- ADU^{-1}, with a mean readout noise of 2.80 ± 0.13 e^-. We obtained one 60 s and two 10 s *V*-band exposures, one 60 s and two 30 s *B*-band exposures, and one 20 s and two 5 s *I*-band exposures for NGC 6318. Figure 1 shows a schematic finding chart of the observed cluster field. The observations were supplemented with a series of 10 bias and 5 dome and sky flat-field exposures per filter during the observing night to calibrate the CCD instrumental signature. Standard stars of selected areas 107 and 110 of Landolt (1992), covering a wide color range, were also observed during the observing night to standardize our photometry. In particular, stars in selected area 110 were observed at low and high air masses in order to properly adjust the extinction coefficients. In total, we obtained 21 different measures of magnitude per filter for the selected standard star sample.

The *BVI* images were reduced at the Instituto de Astronomía y Física del Espacio (IAFE; Argentina) with IRAF[1] using the QUADPROC package. The images were bias-subtracted and flat-fielded by employing weighted combined signal-calibrator frames. In addition, we checked the chip for the existence of any illumination patterns; no correction was necessary. Then the instrumental magnitudes for the standard fields were derived from aperture photometry using DAOPHOT/IRAF routines (Stetson et al. 1990). Since there are as many instrumental magnitudes per filter as observations of standard stars, we used least squares to simultaneously fit the relationships between

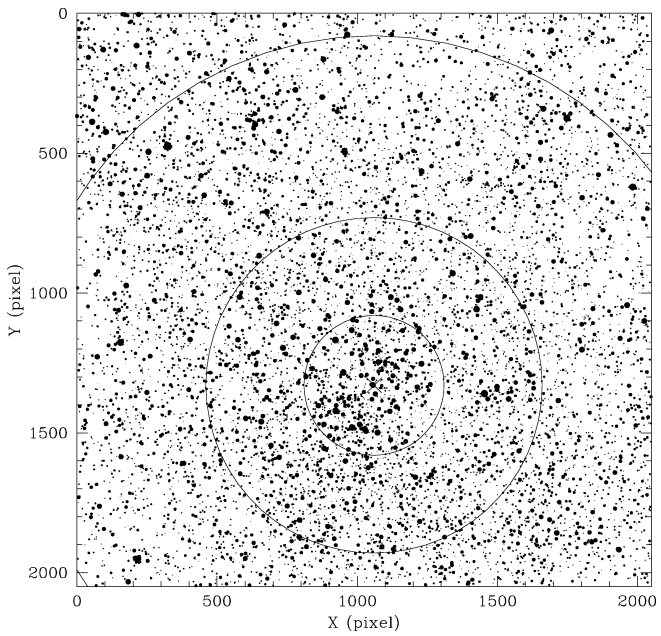

FIG. 1.—Schematic finding chart of the stars observed in the field of NGC 6318. North is up and east is to the left. The sizes of the plotting symbols are proportional to the *V* brightness of the star. Three concentric circles 250, 600, and 1250 pixels wide around the cluster center (*cross*) are also drawn.

instrumental and standard magnitudes, and we obtained the following results:

$$v = (1.844 \pm 0.035) + V + (0.110 \pm 0.026)X_V - (0.027 \pm 0.005)(V - I), \quad (1)$$

$$v = (1.854 \pm 0.034) + V + (0.102 \pm 0.025)X_V - (0.029 \pm 0.005)(B - V), \quad (2)$$

$$b = (1.989 \pm 0.049) + V + (B - V) + (0.249 \pm 0.036)X_B + (0.087 \pm 0.008)(B - V), \quad (3)$$

$$i = (2.694 \pm 0.043) + V - (V - I) + (0.134 \pm 0.032)X_I - (0.023 \pm 0.006)(V - I), \quad (4)$$

where *X* represents the effective air mass. The coefficients were derived through the IRAF routine FITPARAM. Capital and lowercase letters represent standard and instrumental magnitudes, respectively. Note that the instrumental v magnitude was adjusted using both $B - V$ and $V - I$ colors, with the aim of

[1] IRAF is distributed by the National Optical Astronomy Observatories, which is operated by the Association of Universities for Research in Astronomy, Inc., under contract with the National Science Foundation.

TABLE 1
CCD *BVI* DATA OF STARS IN THE FIELD OF NGC 6318

Star	X (pixel)	Y (pixel)	V (mag)	$\sigma(V)$ (mag)	n_V	$B-V$ (mag)	$\sigma(B-V)$ (mag)	n_{B-V}	$V-I$ (mag)	$\sigma(V-I)$ (mag)	n_{V-I}
4365	506.881	1050.924	17.896	0.032	3	1.454	0.102	1	1.876	0.034	3
4366	653.206	1050.924	14.458	0.068	3	1.100	0.015	1	−0.131	2.323	3
4367	1879.611	1050.934	18.498	0.039	3	1.950	0.112	1	2.324	0.041	3
4368	179.225	1051.024	18.208	0.003	3	1.612	0.104	1	1.961	0.069	3
4369	374.110	1051.338	19.639	0.086	3	1.828	0.356	1	2.307	0.125	3

NOTE.—Table 1 is published in its entirety in the electronic edition of the *PASP*. A portion is shown here for guidance regarding its form and content. The (*X*,*Y*) coordinates correspond to the reference system of Fig. 1. Magnitude and color errors are the standard deviations of the mean or, for stars with only one measurement, the observed photometric error.

obtaining one of the two colors for cluster stars not measured in the three filters. The rms error affecting the calibration of equations (1)–(4) are 0.011, 0.011, 0.014, and 0.013 mag, respectively. We then derived the instrumental magnitudes for stars in the NGC 6318 field from point-spread function fits using stand-alone versions of the DAOPHOT[2] and ALLSTAR[2] programs. Before transforming the magnitudes to the standard system, we combined all the independent measurements in three different tables using the stand-alone DAOMATCH[2] and DAOMASTER[2] programs. The columns in these tables list a running number, the X and Y coordinates, the v, b, and i magnitudes, and the respective observational error for each measured star. Once we obtained the standard magnitudes and colors, we built a master table containing the average values of V, $B-V$, and $V-I$, their errors $\sigma(V)$, $\sigma(B-V)$, and $\sigma(V-I)$, and the independent number of observations n_V, n_{B-V}, and n_{V-I} for each star, respectively. Thus, we took advantage of the largest possible amount of information. For example, for a star with three measures in V, one in B, and two in I, we obtained the average of the three values in V, only one $B-V$ value, and the average of two values for $V-I$. This procedure allowed us to keep very blue and very red stars that do not appear in the three filters. Whenever there exists only one measure of V, $B-V$, and/or $V-I$, we adopted the corresponding observational error. We derived magnitudes and colors for 9876 stars in the field of NGC 6318, which are provided in Table 1 (the entire table can be viewed online).

A total of 244 stars observed at CTIO in the BVI_{KC} system were also measured by PBC at Las Campanas Observatory (LCO), and they show good agreement, in general terms. In fact, the mean differences and standard deviations are $V_{CTIO}-V_{LCO}=0.041\pm0.042$, $(B-V)_{CTIO}-(B-V)_{LCO}=-0.036\pm0.060$, and $(V-I)_{CTIO}-(V-I)_{LCO}=-0.012\pm0.042$.

[2] Program kindly provided by P. B. Stetson.

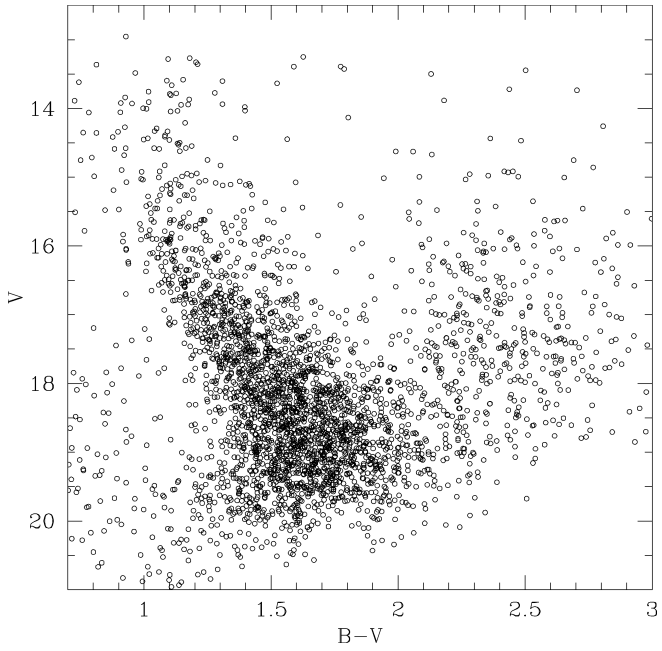

FIG. 2.—(V, $B-V$) CMD for stars observed in the field of NGC 6318.

3. THE (V, $B-V$) AND (V, $V-I$) COLOR-MAGNITUDE DIAGRAMS

Figures 2 and 3 show the resulting (V, $B-V$) and (V, $V-I$) CMDs, respectively, obtained using all the measured stars. A first glance at the figures reveals a crowded broad sequence of stars that traces the cluster main sequence (MS). The blurry q8
appearance of the MS lower and upper envelopes suggests the possible existence of field contamination, differential reddening, or intrinsic dispersion (e.g., binarity, evolutionary effects), or else a combination of all three. Another interesting feature in the (V, $V-I$) CMD is the presence of a redder sequence of stars belonging to the field, which extends from (V, $V-I$) ~ (16, 2.5) down to (21, 3.8). Amazingly, this feature does not have its counterpart in the (V, $B-V$) CMD.

Starting with the examination of the degree of field star contamination in the drawing of a clear fiducial cluster MS, q9
we evaluated such a possibility in the cluster CMDs by first determining the cluster center and then building CMDs of stars distributed in different circular expansions centered on the cluster. The central cluster position was statistically determined

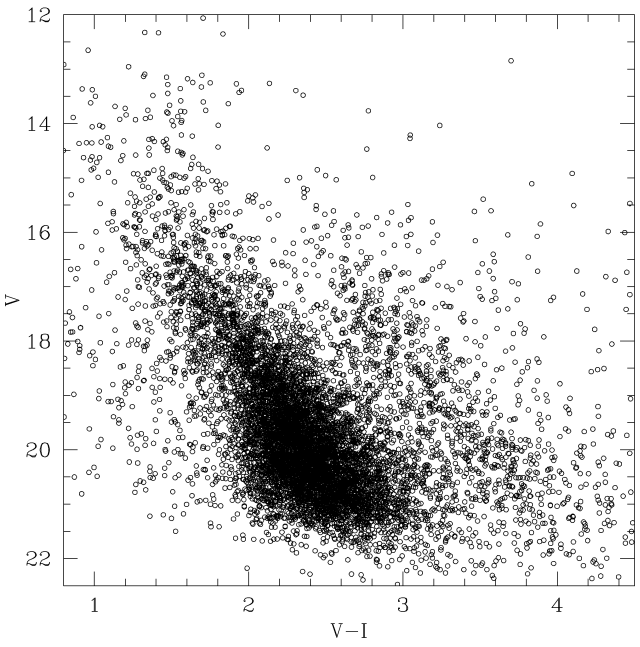

FIG. 3.—(V, $V - I$) CMD for stars observed in the field of NGC 6318.

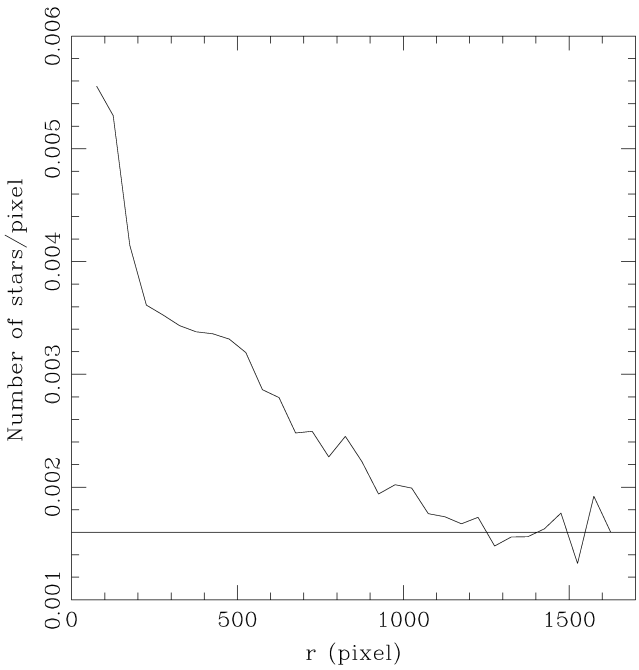

FIG. 4.—Stellar density profile centered at (X_C, Y_C) = (1060, 1330) pixels for stars observed in the field of NGC 6318. The horizontal line represents the background level measured in the field area.

using the stellar density profiles projected onto the directions of the X and Y axes, and by fitting those profiles, we obtained the coordinates associated with the peak of the stellar density distribution. Such profiles were constructed at different size intervals by counting the number of stars distributed along fringes of a fixed width. The width of the fringes in the X and Y directions across the cluster were used to minimize the counting of field stars. The different bin sizes were used to monitor the evolution of the star count noise originating from stellar density fluctuations. The range of useful bin sizes is also constrained by the mean field stellar density, which translates to a lower limit for the mean free path between two stars. In practice, we used bin sizes from 60 to 150 pixel wide and concluded that a 100 pixel wide bin results in a compromise between minimizing the statistical noise—mainly caused by the presence of localized groups, rows, or columns of stars—and maximizing the spatial resolution.

The projected stellar density profiles were fitted using the NGAUSSFIT routine within the IRAF/STSDAS package. We chose the multiple Gaussian fitting option and fixed the constant and linear terms to the corresponding background level and to zero, respectively, and set the number of matching Gaussians to one. The amplitude, FWHM, and the center of the Gaussian acted as variables. We iterated the fitting procedure once on average, after eliminating a couple of dispersed points. The final coordinates for the cluster center turned out to be (X_C, Y_C) = (1060 ± 20, 1330 ± 30) pixels, which we adopted in the analysis that follows. The cluster center is marked by a cross in Figure 1. We also derived the FWHMs of the projected stellar density profiles. We obtained $\sigma(X) = 590 \pm 30$ pixels and $\sigma(Y) = 620 \pm 60$ pixels for the half-widths at half-maximum of the projected Gaussians in the X and Y directions, respectively.

We then built the cluster radial profile, from which we estimated the cluster radius, which is generally used as an indicator of the cluster dimensions, and established the area over which field stars practically prevail. The availability of a field area is highly valued, mainly because of the advantages it presents in disentangling fiducial cluster and field features in the observed CMDs. Cluster stellar density radial profiles are usually built by counting the number of stars distributed in concentric rings around the cluster center and normalizing the sum of stars in each ring to the unit area. This procedure allows us to stretch the radial profile to its utmost, until complete circles can be traced in the observed field. However, in order to move even farther away from the cluster center, we decided to follow another method based on counts of stars located in boxes 50 pixels on a side, distributed throughout the whole field. Thus, the number of stars per unit area at a given radius r can be directly calculated through the expression

$$(n_{r+25} - n_{r-25})/[(m_{r+25} - m_{r-25}) \times 50^2],$$

where n_j and m_j represent the number of counted stars and boxes included in a circle of radius j, respectively. Note that the method does not necessarily require a complete circle of radius r within the observed field to be able to estimate the

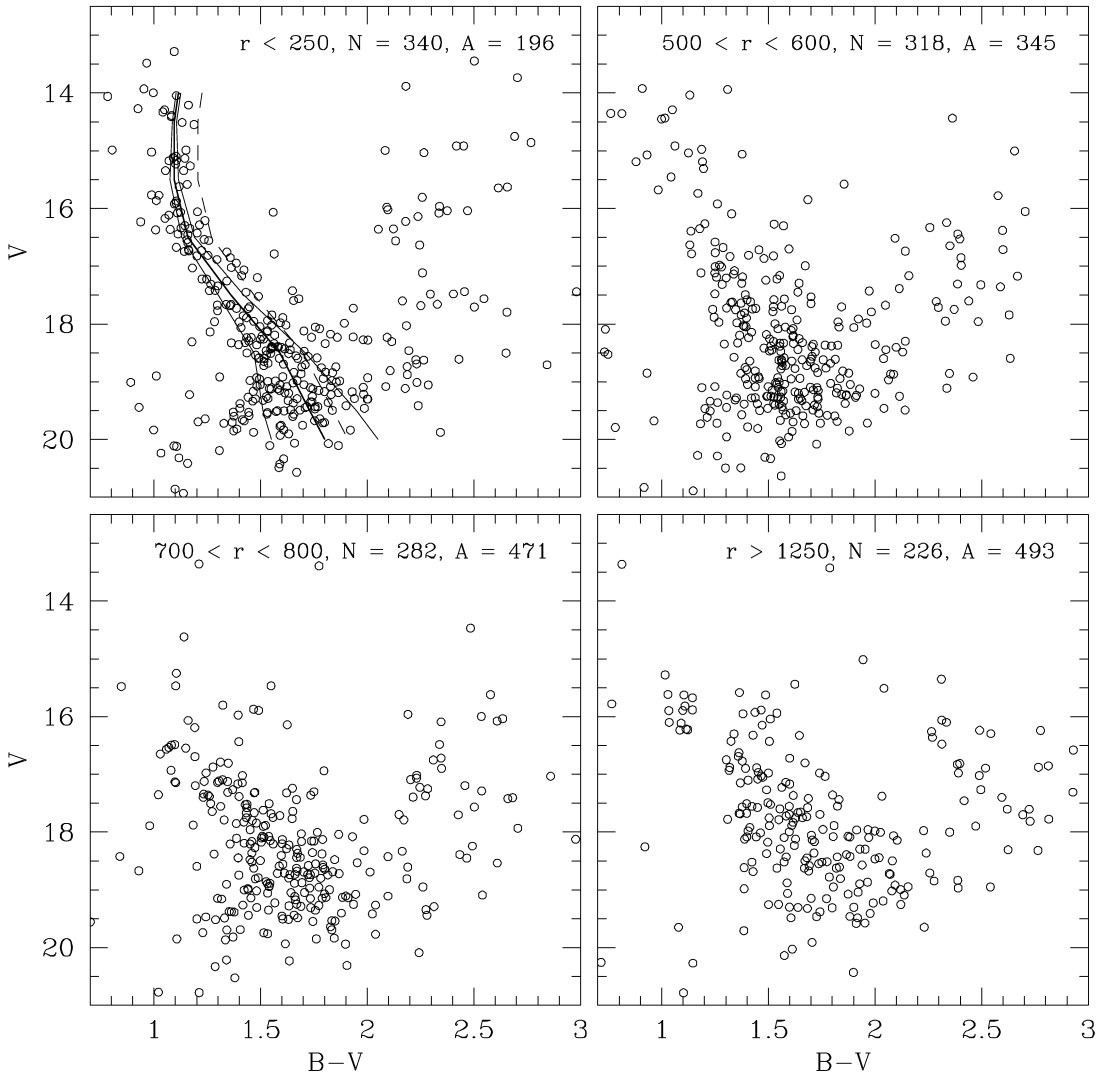

FIG. 5.—($V, B - V$) CMD for stars observed in different extracted circular regions around the cluster center as indicated in each panel, along with the corresponding number of stars and the covered area in units of $10^3 \times$ pixels^2. *Top left*: The fiducial cluster MS, the $\pm 1 \times \sigma(B - V)$ shifted MSs, and the Burki's limit-shifted MS are overplotted (see § 3 for details).

mean stellar density at that distance. What is more, instead of having traced the radial profile of NGC 6318 out to $r \sim 700$ pixels (the radius of the largest complete circle that can be traced in the observed field), we obtained a cluster stellar density profile that extends beyond $r \sim 1600$ pixels from its center, as is shown in Figure 4. The horizontal line represents the background level measured for $r > 1300$ pixels. This mean field density is ~3.5 times lower than the central cluster density. The half-maximum and cluster radius were estimated at $r = 250$ and 1250 pixels, respectively. Therefore, we adopted 1250 pixels, which is equivalent to ~8′, as the cluster angular radius.

Figures 5 and 6 show four CMDs extracted from three circular regions centered on the cluster and from the surrounding field ($r > 1250$ pixels), respectively. The radii of the circular extractions were chosen using the stellar density profile of Figure 4 as reference. The extracted regions are labeled at the top of each panel, along with the corresponding number of stars (N) and the covered area (A) in units of $10^3 \times$ pixels^2. The top left panel clearly shows the cluster fiducial MS, whereas in the bottom right panel the cluster features are practically absent. In the top right panel, some trails of cluster MS stars still appear, while the bottom left panel is dominated by field stars. Both CMDs provide detailed information about the cluster-field transition region. While the top right CMD insinuates a relatively crowded field star sequence superimposed onto the cluster MS, the bottom left panel reveals the existence of a composite field in the CMD, dominated by intermediate-age and young disk stars. The field MS shown in the bottom right

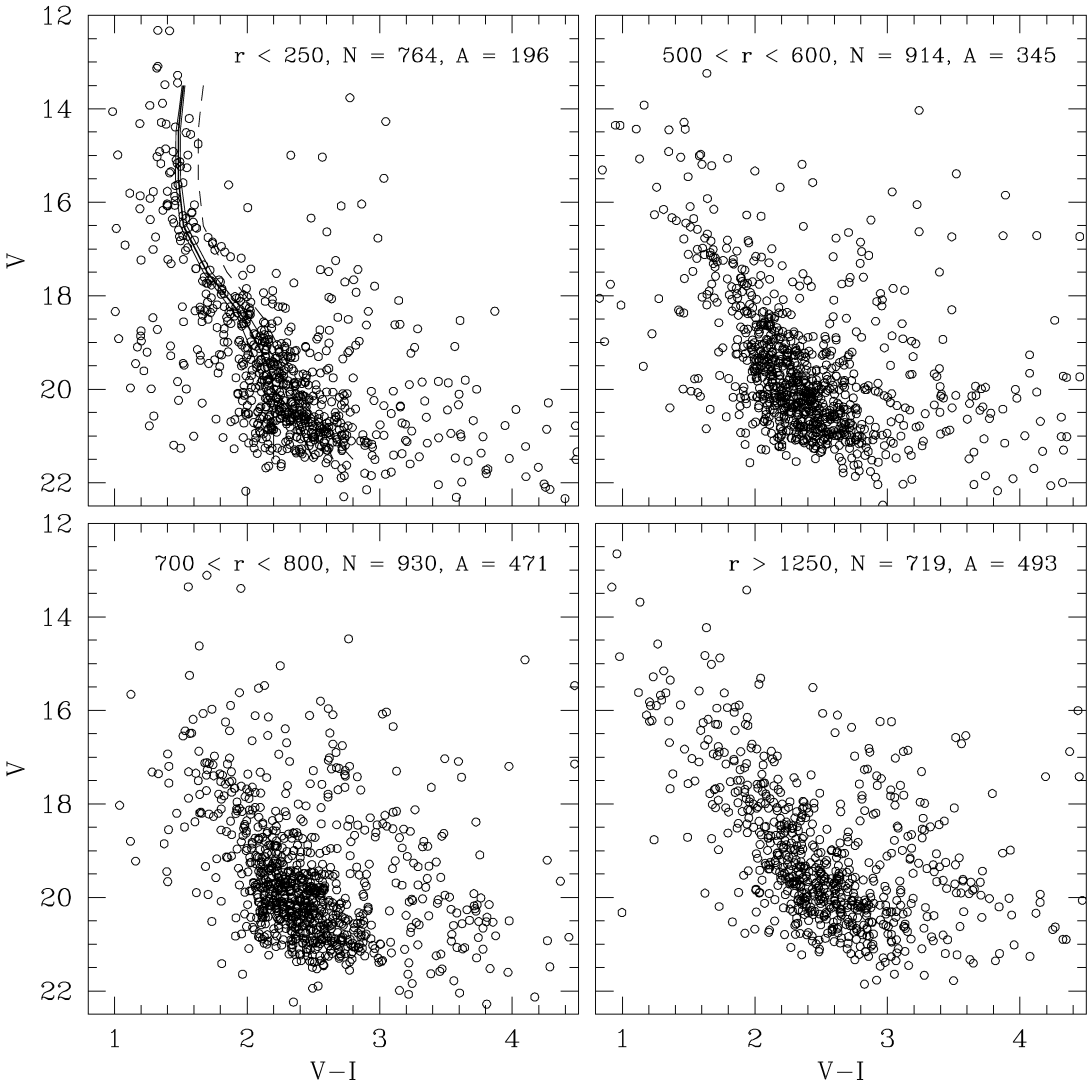

FIG. 6.—(V, $V-I$) CMD for stars observed in different extracted circular regions around the cluster center as indicated in each panel, along with the corresponding number of stars and the covered area in units of $10^3\times$ pixels^2. *Top left*: The fiducial cluster MS, the $\pm 1 \times \sigma(V-I)$ shifted MSs, and the Burki's limit-shifted MS are overplotted (see § 3 for details).

panel is located to the right of the cluster MS ($r < 250$ pixels), which means that although NGC 6318 appears to be highly reddened, some observed field stars should be located even farther behind the cluster. In particular, the redder star sequence in the bottom right panel corresponds to inner disk horizontal branch stars affected by different amounts of interstellar reddening (Ng et al. 1996).

We looked into the nature of the broadness of the cluster MS ($r < 250$ pixels) by examining the distribution of stars located at different distances from the fiducial cluster MS. First, we defined the fiducial cluster MS as the curve that joins the points on the cluster MS and has the highest star densities. Thick solid lines in the top left panels of Figures 5 and 6 indicate the resulting fiducial sequences. Second, we defined the cluster MS width due to photometric error as the distance between points that are separated by $\sigma(B-V)$ and $\sigma(V-I)$ from the fiducial cluster MSs, respectively, at any V magnitude level. The values of $\sigma(B-V)$ and $\sigma(V-I)$ were taken from Table 2. Thin solid lines in the top left panels of Figures 5 and 6 on both sides of the fiducial cluster MSs represent the lower and upper limits of the defined MS widths. Third, we shifted the fiducial cluster MSs redward until we reached the lower limit estimated by Burki (1975) for clusters with differential reddening: $\Delta(B-V) = 0.11$, which corresponds to $\Delta(V-I) = 0.15$ if a value of 1.33 for the $E(V-I)/E(B-V)$ ratio (Cousins 1978) is adopted. These curves are marked in the top left panels of Figures 5 and 6 by short dashed lines. As can be seen, neither photometric errors nor differential reddening seem to

TABLE 2
MAGNITUDE AND COLOR PHOTOMETRIC ERROR AS A FUNCTION OF V

ΔV (mag)	$\sigma(V)$ (mag)	$\sigma(B-V)$ (mag)	$\sigma(V-I)$ (mag)
<12	0.010	<0.010	0.010
12–13	0.010	<0.010	0.010
13–14	0.010	0.010	0.010
14–15	0.015	0.010	0.015
15–16	0.015	0.015	0.020
16–17	0.020	0.015	0.025
17–18	0.025	0.030	0.030
18–19	0.035	0.080	0.045
19–20	0.050	0.220	0.080
20–21	0.090	...	0.140
21–22	0.220	...	0.300

TABLE 3
FUNDAMENTAL PARAMETERS OF CLUSTERS LOCATED TOWARD NGC 6318

Name	l (deg)	b (deg)	$E(B-V)$ (mag)	d (kpc)
NGC 6231	343.46	1.18	0.44	1.2
Trumpler 24	344.70	1.50	0.42	1.1
NGC 6322	345.28	−3.06	0.59	1.0
NGC 6242	345.47	2.47	0.38	1.1
NGC 6268	346.05	1.30	0.39	1.0
NGC 6281	347.73	1.97	0.15	0.5
HM 1	348.70	−0.77	1.85	2.9
BH 222	349.13	−0.44	1.85	6.0
Bochum 13	351.20	1.36	0.85	1.1
Ruprecht 127	352.88	−2.50	0.99	1.5

be responsible for the broadness of the cluster MS. We conclude that a more probable factor for the MS blurring is contamination by field stars.

A simple inspection of the photometric data shows that 81% of the stars in the top left panel of Figure 5 have three measures of their V magnitudes and $B-V$ colors and extend approximately along the whole magnitude range, while 10% and 9% of the stars have two and one measure, respectively, and cover V ranges from 19.5 to 20 mag. For the top left panel of Figure 6, 45%, 16%, and 39% of the stars have three, two, and one measure and extend from the brightest limit down to $V = 20$, from 19 to 21, and from 20 until the photometric limit, respectively. Thus, stars with three measures that also have smaller photometric errors become a valuable reference for the reliability of the morphology and position of the cluster MS.

The different field features identified in the bottom right panels of Figures 5 and 6 are not recognized at all in the 600 pixel $< r <$ 700 pixel CMDs at all, as would be expected if the field had a relatively homogeneous stellar composition. For example, field MS stars brighter than $V \sim 17$ are mainly seen in the CMDs in the bottom right panels. This suggests that the field stellar composition varies across the observed sky area. For this reason, instead of carrying out a statistical field subtraction using the $r > 1250$ pixel CMDs as reference, we decided to consider the innermost extracted CMDs as representative of the cluster CMDs, and hence to estimate its fundamental parameters. In addition, and in order to obtain a better definition of the upper cluster MS and red, evolved features, we combined the $r < 250$ pixel CMDs with all the stars observed with $V < 14$, $B-V > 1.0$, and $V-I > 1.3$.

4. FUNDAMENTAL PROPERTIES OF NGC 6318

The widely used procedure of fitting theoretical isochrones to observed CMDs was employed to estimate the $E(B-V)$ and $E(V-I)$ color excesses, the $V-M_V$ apparent distance modulus, and the age and the metallicity of NGC 6318. We fitted theoretical isochrones computed by Lejeune & Schaerer (2001) to the observed $(V, B-V)$ and $(V, V-I)$ CMDs. The isochrones, which cover the age range from 10^3 yr to 16–20 Gyr in steps of $\Delta \log t = 0.05$ dex, were calculated for the entire set of nonrotating Geneva stellar evolution models, covering masses from 0.4–0.8 to 120–150 $M_\odot$ and metallicities from $Z = 0.0004$ to 0.1. When selecting subsets of isochrones for different Z values to address the metallicity effect in the cluster fundamental parameters, we preferred those that include overshooting effects, even though we initially decided to use solar ($Z = 0.020$) and subsolar ($Z = 0.008$) chemical compositions for the isochrone sets.

First, we independently fitted the zero-age main sequence (ZAMS) to the $(V, B-V)$ and $(V, V-I)$ CMDs for each selected metallicity and derived the cluster color excesses $E(B-V)$ and $E(V-I)$ and the apparent distance modulus $V-M_V$. The relatively long observed cluster MS allowed for these parameters to be accurately determined. Note that $B-V$ and $V-I$ colors are not metallicity indicators. However, while $V-I$ is virtually free of metallicity effects, $B-V$ exhibits some signs of small metallicity sensitivity. For that reason, differences in color excesses and apparent distance modulus for $Z = 0.020$ and 0.008 are mainly reflected in the $(V, B-V)$ CMD. Still, the differences for these parameters between both metallicities result within 1 σ of the derived parameter errors. Second, we selected isochrones some hundred million years old and used the derived pairs of $(V-M_V, E[B-V])$ and $(V-M_V, E[V-I])$ values to estimate the cluster age. Finally, we compared the best fits obtained from the two different metallicities and chose the one that best resembled the cluster MS, particularly the upper MS region. Bearing in mind the broadness of the cluster MS, we did not find any advantage in choosing one of the selected metallicities over another. However, we favor the solar abundance value, since one should expect it for a cluster that is some hundred million years old and located toward the Galactic center (see, e.g., Piatti et al. 1995; Twarog et al. 1997; Friel et al. 2002; Chen et al. 2003). Therefore, the isochrone of $\log t = 8.20$ ($t = 160$ Myr) and $Z = 0.020$ turned out to be the one that most accurately reproduces the cluster features in the $(V, B-V)$ and $(V, V-I)$ CMDs. To match this isochrone, we used $E(B-V)$ and $E(V-I)$ color excesses and

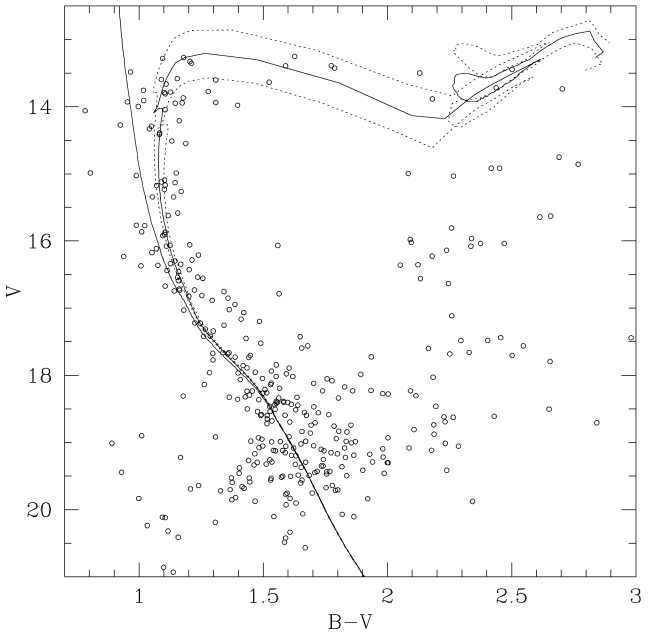

FIG. 7.—Composite (V, $B-V$) CMD of NGC 6318. Overplotted are the ZAMS and the isochrones for $\log t = 8.10$, 8.20, and 8.30 ($Z = 0.020$) from Lejeune & Schaerer (2001), taking into account overshooting.

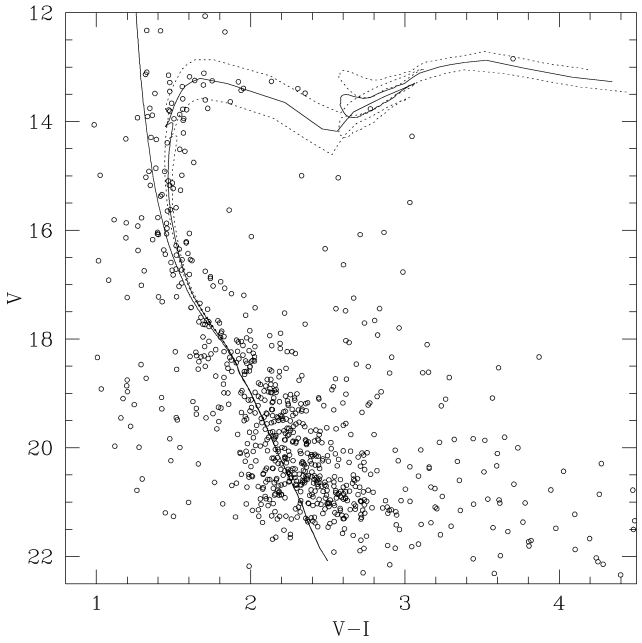

FIG. 8.—Composite (V, $V-I$) CMD of NGC 6318. Overplotted are the ZAMS and the isochrones for $\log t = 8.10$, 8.20, and 8.30 ($Z = 0.020$) from Lejeune & Schaerer (2001), taking into account overshooting.

a $V - M_V$ apparent distance modulus of 1.20, 1.55, and 15.45, respectively, which were derived from the ZAMS fit. The uncertainties of these parameters were estimated from the individual values obtained from the cluster feature dispersion. Thus, we estimated $\sigma(E[B-V]) = 0.05$ and $\sigma(E[V-I]) = 0.10$ mag, $\sigma(V - M_V) = 0.35$ mag, and $\sigma(t) = {}^{+40}_{-30}$ Myr. In Figures 7 and 8 we overlapped the ZAMS and the isochrone of $\log t = 8.20$ (*solid lines*) for $Z = 0.020$ to the cluster CMDs, and two additional isochrones of $\log t = 8.10$ and 8.30 for comparison purposes (*dotted lines*). PBC obtained $E(B-V)$ and $E(V-I)$ color excesses and a $V - M_V$ distance modulus in excellent agreement with the above results, but dated NGC 6318 as an open cluster 8 times younger ($t = 20 \pm 10$ Myr) than the present cluster age. Their cluster age, however, relies on the fitting of empirical isochrones onto the V versus $V - I$ CMD, on the Balmer absorption line equivalent widths—which were calibrated in terms of age by Bica & Alloin (1986, 1987)—and on the matching of the cluster integrated spectrum with age-templated spectra. While their less well defined cluster MS explains the smaller age value (see their Fig. 4), the contamination by field stars into the cluster integrated light could result in a bluer (younger) spectrum. Now, with a more rigorous treatment of the photometric outliers, we traced better fiducial cluster sequences, which allowed us to make a more reliable cluster age estimate.

The possibility of estimating $E(B-V)$ and $E(V-I)$ independently allowed for its ratio to be computed, resulting in $E(V-I)/E(B-V) = 1.29 \pm 0.16$. When comparing this value with that coming from the normal interstellar extinction law (1.33; Cousins 1978), we found excellent agreement. Therefore, we used the derived reddenings and apparent distance modulus and the most frequently used values for the $A_V/E(B-V)$ ratio (Cousins 1978) to obtain $V_0 - M_V = 11.6 \pm 0.5$, which implies a distance from the Sun of 2.1 ± 0.5 kpc. The distance error was computed with the expression $\sigma(d) = 0.46\,[\sigma(V - M_V) + 3.2\,\sigma(E[B-V])]\,d$, where $\sigma(V - M_V)$ and $\sigma(E[B-V])$ represent the estimated errors in $V - M_V$ and $E(B-V)$, respectively. By using the cluster Galactic coordinates (l, b) and the calculated distance, we derive 6.45, -0.44, and -0.03 kpc for its X, Y, and Z coordinates, respectively, assuming the Sun's distance from the center of the Galaxy to be 8.5 kpc.

The availability of recent compilations of fundamental parameters of open clusters (see, e.g., Dias et al. 2002; Chen et al. 2003) allowed us to place the present results for NGC 6318 in the context of the Galactic structure. As far as we are aware, the WEBDA open cluster database[3] offers a favorable image of the available data, since it is updated periodically. Thus, we searched WEBDA for open clusters with well-determined interstellar reddenings $E(B-V)$ and distances from the Sun. We required that for a cluster to be included in the output list, $(l, b)_{\rm cluster} = (l, b)_{\rm NGC\ 6318} \pm 5°$ in order to investigate the struc-

[3] See http://obswww.unige.ch/webda/navigation.html.

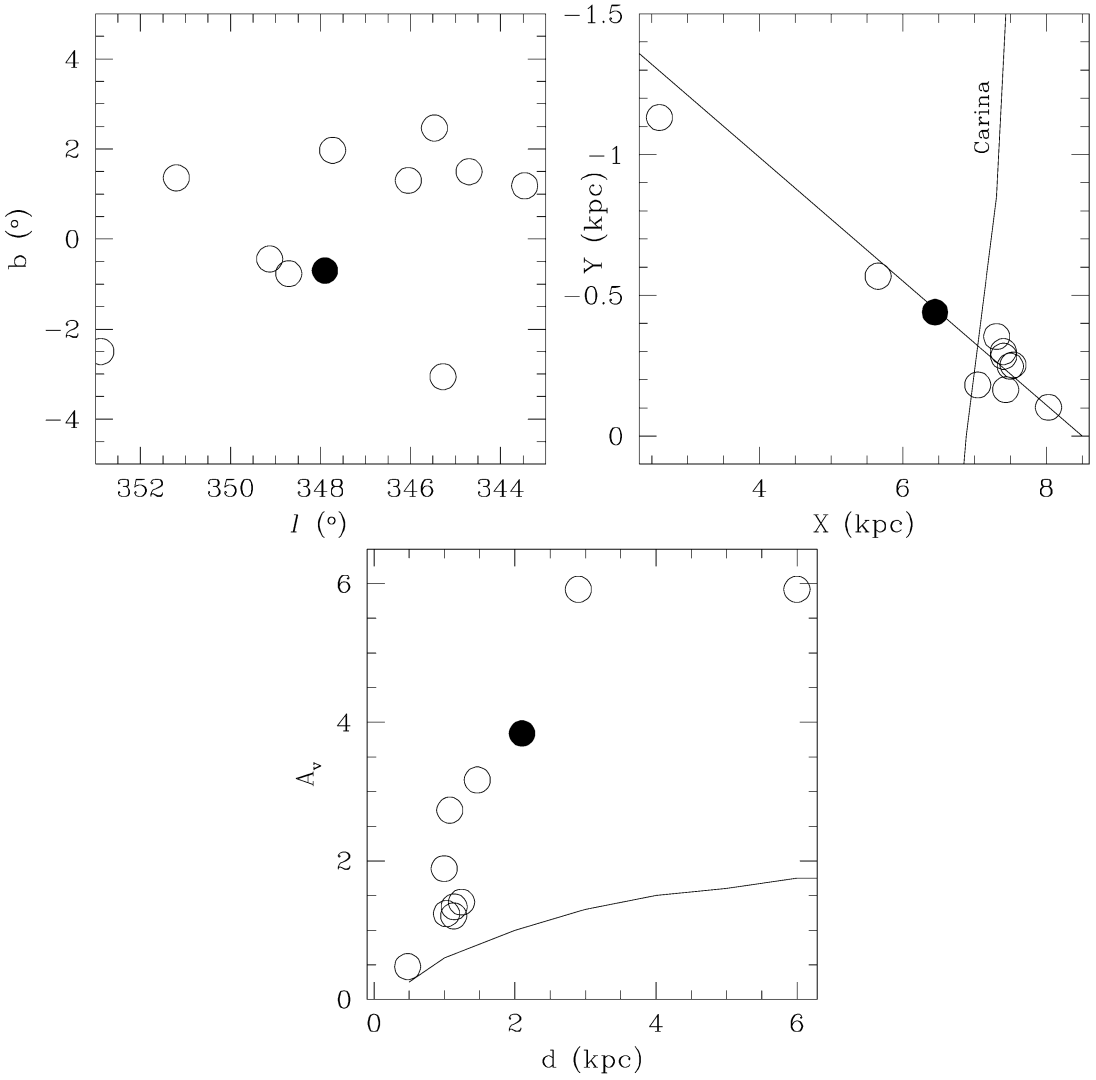

FIG. 9.—*Top left*: Galactic coordinates (*l*, *b*) of open clusters studied within a field 10° × 10° around NGC 631. *Top right*: The Galactic plane with the (*X*, *Y*) positions of these clusters and the line of sight from the Sun to NGC 6318 and the Carina spiral arm are superimposed. *Bottom*: The visual interstellar absorption A_V vs. the cluster distance *d* from the Sun and the relation for the Baade's window are also superimposed. NGC 6318 is drawn with a filled circle in all panels. See details in § 4.

ture of the Galactic disk along the line of sight of NGC 6318. Finally, we found 10 clusters that fulfill the required conditions.

The top left panel of Figure 9 shows the (*l*, *b*) plane, with the selected clusters and NGC 6318 represented by open circles and a filled circle, respectively. It can be inferred from this figure that all these clusters are located close to the Galactic plane. The distribution of the selected objects in the Galactic plane is depicted in the top right panel, which shows the clusters aligned along the line of sight of NGC 6318, as seen from the Sun. Note that the distance between the outermost and innermost clusters is more than 5 kpc and that NGC 6318 is located behind the Carina spiral arm. The bottom panel shows the relationship between the visual interstellar absorption A_V and the distance *d* from the Sun. For the sake of comparison, we also included the relationship for the Baade's window ($[l, b] = [1°, -3.^\circ 9]$) obtained by Ng et al. (1996), which is represented by the solid line. A close inspection of this figure allowed us to note the following features: (1) HM 1 and BH 222 are the farthest open clusters of the sample, located at 2.9 and 6.0 kpc from the Sun, respectively. However, in spite of being separated by more than 3 kpc, they are surprisingly affected by the same visual absorption. On the other hand, note that at the BH 222 distance, the visual absorption toward the Baade's window—not too far from the direction of NGC

6318—is ~4 mag smaller. (2) Open clusters located between ~1 and 2 kpc from the Sun exhibit slightly higher visual absorption than those expected for a quasi-linear extinction law. It would be interesting to investigate whether this effect can be attributed to the presence of the Carina spiral arm.

5. CONCLUSIONS

CCD BVI_{KC} photometry of 9876 stars in the field of the southern open cluster NGC 6318 (BH 218) is reported here. The present data supersede that reported previously by PBC, thus allowing us to extend the corresponding cluster MS ~2 mag fainter than that obtained by PBC. It is shown that neither photometric error nor differential reddening are the responsible for the observed broadness of the cluster MS, the more probable cause of the MS blurring being the contamination by field stars. An examination of the observed CMDs shows that NGC 6318 is a young, highly reddened open cluster located beyond the Carina spiral feature. For $Z = 0.020$, the best-fitting isochrones of the Geneva group yield $E(B - V) = 1.20 \pm 0.05$, $E(V - I) = 1.55 \pm 0.10$, and $V - M_V = 15.45 \pm 0.35$, and an age of 160 Myr. Therefore, NGC 6318, located 2.1 ± 0.5 kpc from the Sun and 30 pc below the Galactic plane, is now found to be significantly older than previously believed. A cluster angular radius of 8′ (equivalent to a linear radius of 5 pc) was estimated from star counts performed within and outside of the cluster area. An inspection of the properties of 10 known open clusters aligned along the line of sight of NGC 6319 as seen from the Sun reveals that two open clusters (HM 1 and BH 222) are the farthest ones, while those located between 1 and 2 kpc from the Sun are somewhat more absorbed than those expected to follow a quasi-linear extinction law.

We are gratefully indebted to the CTIO staff for their hospitality and support during the observing run. We also thank an anonymous referee, whose comments helped us to improve the manuscript. This work was partially supported by the Argentinian institutions CONICET, SECYT (Universidad Nacional de Córdoba), Agencia Córdoba Ciencia, and Agencia Nacional de Promoción Científica y Tecnológica (ANPCyT). This work was based on observations made at Cerro Tololo Inter-American Observatory, which is operated by AURA, Inc., under cooperative agreement with the NSF.

REFERENCES

Archinal, B. A., & Hynes, S. J. 2003, Star Clusters (Richmond: Willman-Bell)
Bica, E., & Alloin, D. 1986, A&A, 162, 21
———. 1987, A&A, 186, 49
Burki, G. 1975, A&A, 43, 37
Chen, L., Hou, J. L., & Wang, J. J. 2003, AJ, 125, 1397
Collinder, P. 1931, Ann. Obs. Lund, 2, 1
Cousins, A. W. J. 1978, Mon. Notes Astron. Soc. South Africa, 37, 62
Dias, W. S., Alessi, B. S., Moitinho, A., & Lépine, J. R. D. 2002, A&A, 389, 871
Friel, E. D., Janes, K. A., Tavarez, M., Scott, J., Katsanis, R., Lotz, J., Hong, L., & Miller, N. 2002, AJ, 124, 2693
Landolt, A. U. 1992, AJ, 104, 340
Lauberts, A. 1982, The ESO/Uppsala Survey of the ESO(B) Atlas (Garching: ESO)
Lejeune, T., & Schaerer, D. 2001, A&A, 366, 538
Melotte, P. J. 1915, MmRAS, 60, 175
Mermilliod, J.-C. 2004, WEBDA Open Cluster Database, http://obswww.unige.ch/webda
Ng, Y. K., Bertelli, G., Chiosi, C., & Bressan, A. 1996, A&A, 310, 771
Piatti, A. E., Bica, E., & Clariá, J. J. 2000a, A&A, 362, 959 (PBC)
Piatti, A. E., & Clariá, J. J. 2002, A&A, 388, 179
Piatti, A. E., Clariá, J. J., & Abadi, M. G. 1995, AJ, 110, 2813
Piatti, A. E., Clariá, J. J., & Ahumada, A. V. 2003, MNRAS, 340, 1249
———. 2004, MNRAS, 349, 641
Piatti, A. E., Clariá, J. J., & Bica, E. 2000b, A&A, 360, 529
Stetson, P. B., Davis, L. E., & Crabtree, D. R. 1990, in ASP Conf. Ser. 8, CCDs in Astronomy (San Francisco: ASP), 289
Trumpler, R. J. 1930, Lick Obs. Bull., 14, 154
Twarog, B. A., Ashman, K. M., & Anthony-Twarog, B. J. 1997, AJ, 114, 2556
van den Bergh, S., & Hagen, G. J. 1975, AJ, 80, 11

QUERIES TO THE AUTHOR

1 Au: PASP follows American usage of ″that″ to introduce restrictive clauses, ″which″ for nonrestrictive. Changes have been noted as ″that/which.″

2 Au: Cluster directions are using Julian equinox, correct (i.e., J2000.0)?

3 Au: PASP observes conservative grammar conventions; here and throughout, ″due to″ changed where phrase modifies verb.

4 Au: Does sentence wording accurately reflect your intended meaning? (″In this work...″ plus following sentences)

5 Au: Does sentence wording accurately reflect your intended meaning? (″The *BVI* images...″)

6 Au: Does sentence wording accurately reflect your intended meaning? (″Since there are as many instrumental magnitudes...″)

7 Au: PASP does not use explicit multiplication signs (dots, asterisks, or crosses) except in scientific notation. They have been omitted here.

8 Au: that/which

9 Au: Does sentence wording accurately reflect your intended meaning? (″Starting with the examination...″)

10 Au: Does sentence wording accurately reflect your intended meaning? (″Such profiles were constructed...″)

11 Au: that/which

12 Au: that/which

13 Au: Does sentence wording accurately reflect your intended meaning? (″The half-maximum and cluster radius...″)

14 Au: that/which

15 Au: Table 3 was not mentioned in the text. Please provide instructions for placing a reference to this table.

16 Au: that/which

17 Au: Figure 7 & 8 legends: Does sentence wording accurately reflect your intended meaning? (″Overplotted are the ZAMS...″)

18 Au: The sigma notation her, while correct, is uncommon. Please double−check this for accuracy.

19 Au: PASP style is to place URLs in footnotes rather than the body of the text. A footnote containing the information has been provided.

2005 PAGE CHARGES/REPRINT PRICES

New : 2% discount on payment made within 30 days of invoice date!

AUTHORS: This form should be used to calculate page charges, color-printing costs, and reprint costs. Payment by check, Money Order, Visa, or MasterCard is required with all orders not accompanied by an institutional purchase order or purchase order number. **Make checks and purchase orders payable to The University of Chicago Press.**

PAGE CHARGES FOR PASP:

Type of Charge	Charge
Electronic manuscript in latex	$110 per page
Paper manuscript and non-latex e-files	$150 per page
Invited Review Papers	$60 per page
Color figure(s) in the print edition	$150 per color figure
Machine readable data table to appear in electronic edition only*	$110 per table
Author alterations	$6 per change

REPRINT CHARGES:

Please use the following chart to determine the cost of your reprints. Reprint orders will not be accepted without proof of payment of page charges. No free reprints are provided, and no reprints may be ordered when page charges have been waived. The minimum order is **50** copies. Please indicate the quantity desired by each author along with shipping and billing addresses in the spaces provided. Reprints are shipped free of charge. Please allow 4**-6** weeks after publication for delivery. Faster delivery can be arranged at the author's expense; please contact the billing coordinator.

	TOTAL QUANTITY				
	50	**100**	**150**	**200**	**ADD'L 50**
# OF PAGES					
1-4	$88	$92	$97	$103	$21
5-8	$110	$121	$133	$145	$31
9-12	$143	$155	$167	$178	$40
13-16	$176	$188	$200	$212	$51
17-20	$209	$221	$233	$244	$62
21-24	$242	$254	$266	$278	$72
25-28*	$275	$288	$300	$312	$80
COVERS	$79	$88	$97	$101	$17

*For articles with a larger number of pages, combine rates (e.g., 36 pages =28+8, 50 reprints will cost $275+$110=$385)

• If more than two institutions are paying page charges, please submit information on a separate sheet attached to this form.
• If page charges are to be paid from funds with a specific expiration date and early billing is necessary, please request advance billing from the billing coordinator at least 30 days prior to the expiration date. The billing amount will be based on an estimate of paper length. Extensive additions or alterations to any paper that is prebilled could result in higher costs, depending on the nature of the changes.

If payment is to be made by purchase order: reprint payment, color charges, and page charges can ALL be included on a single purchase order.*

Publications of the Astronomical Society of the Pacific

The University of Chicago Press
1427 E. 60th Street
Chicago, IL 60637
FAX (773) 753-3616

2% discount on payment made within 30 days of

❑ NO REPRINTS DESIRED

2005 PAGE CHARGE / REPRINT ORDER FORM

(Please keep a copy of this document for your records)

AUTHORS: Please return this form immediately **even if no reprints are desired**.

- Use this form to order reprints and allocate cost of page charges, color printing costs, and reprints.
- Payment can be made by institutional purchase order or purchase order number, check, wire transfer, Visa or MasterCard.
- Reprints ordered through an institution will not be processed without a purchase order number or other payment arrangements.
- All purchase orders MUST include journal name and date of issue, authors' names, title of article, and number of reprints ordered.
- **MAKE CHECKS AND PURCAHSE ORDERS PAYABLE TO The University of Chicago Press.**
- Direct billing questions to **Cindy Garrett,** Billing Coordinator, (773) 753-8028; fax (773) 753-3616; Astronomy-Billing@press.uchicago.edu.

Publications of the Astronomical Society of the Pacific Vol. _____ No. _____ Issue _____

Title of Article _____

Author Name(s) _____

Estimated No. of Pages _____ Manuscript No. _____ No. of Color Figures to Appear in Print _____

Number of machine-readable tables _____ On-line Materials _____

Contact _____ Phone/fax/e-mail _____

SIGNATURE OF ADMINISTRATIVE OFFICIAL _____

PAGE CHARGES Invoice(s) to be sent to the following address(es)

_____% to be paid by

_____

_____

_____

PAYMENT OPTIONS

1) Inst'l. Purchase Order No. _____

Purchase Order attached ❑ or to come ❑

Funding Account or Grant No. _____

2) ❑ Check or money order for total charges is attached

3) Credit Card: ❑ VISA ❑ MasterCard ❑ AMEX ❑ Discover

4) ❑ Wire Transfer

Card No. _____ Exp. date. _____

SIGNATURE _____

Phone No. _____

Invoice(s) to be sent to the following address(es)

_____% to be paid by

_____

_____

_____

PAYMENT OPTIONS

1) Inst'l. Purchase Order No. _____

Purchase Order attached ❑ or to come ❑

Funding Account or Grant No. _____

2) ❑ Check or money order for total charges is attached

3) Credit Card: ❑ VISA ❑ MasterCard ❑ AMEX ❑ Discover

4) ❑ Wire Transfer

Card No. _____ Exp. date. _____

SIGNATURE _____

Phone No. _____

REPRINT CHARGES

Quantity_____ ❑ without covers ❑ with covers

Ship reprints to _____

_____

_____

Send invoices to _____% to be paid by

_____

_____

_____

PAYMENT OPTIONS

1) Institutional Purchase Order No. _____

Purchase Order attached ❑ to come ❑

2) ❑ Check ❑ Wire transfer

3) Credit card to be used as: ❑ proof of payment **OR** ❑ payment

Credit Card: ❑ VISA ❑ MasterCard ❑ AMEX ❑ Discover

Card No. _____ Exp. Date _____

SIGNATURE _____

Phone No. _____

REPRINT CHARGES

Quantity_____ ❑ without covers ❑ with covers

Ship reprints to _____

_____

_____

Send invoices to _____ _____% to be paid by

_____

_____

_____

PAYMENT OPTIONS

1) Institutional Purchase Order No. _____

Purchase Order attached ❑ to come ❑

2) ❑ Check ❑ Wire transfer

3) Credit card to be used as: ❑ proof of payment **OR** ❑ payment

Credit Card: ❑ VISA ❑ MasterCard ❑ AMEX ❑ Discover

Card No. _____ Exp. Date _____

SIGNATURE _____

Phone No. _____

2005 PUBLICATION AGREEMENT AND COPYRIGHT ASSIGNMENT

Publications of the Astronomical Society of the Pacific

Publisher: University of Chicago Press, 1427 East 60th Street., Chicago, IL 60637

Date: _____

Manuscript number-_____ (please fill in) Issue date: _____

With regard to the original and previously unpublished paper entitled, " _____
_____ "
by _____
the following terms are submitted for your consideration. If these terms are satisfactory, please sign below and return this agreement to the University of Chicago production office. We will not publish your paper without this approval.

Copyright Assignment: Because the Astronomical Society of the Pacific (ASP) is undertaking to publish this paper, and because you desire to have this paper so published, you grant and assign the entire copyright for this paper exclusively to the ASP. The copyright consists of all rights protected by the original copyright laws of the United States and of all foreign countries, in all languages and forms of communication.

The ASP, in return, grants to you the non-exclusive right of publication, subject only to your giving appropriate credit to the *Publications*. To protect the copyright in this paper, the original copyright notice as it appears in the *Publications* should be included in the credit.

Compensation and Subsidiary Rights: It is understood that you will receive no monetary compensation from the ASP for the assignment of copyright and publication of the paper. Please note, however, that you may grant or deny requests to reprint this paper in books or journals, and you may retain all fees from such reprinting. We will forward such requests to you.

Who Should Sign: The agreement should be signed by at least one of the authors (who agrees to informs the others, if any) or, in the case of a "work made for hire," by the employer.

An author who is a U.S. Government officer or employee and who prepared the paper as a part of his or her official duties does not own any copyright in it. If at least one of the authors is not in this category, that author should sign below. If all the authors are in this category, please check the box below and return this form unsigned.

Anne P. Cowley
F. David A. Hartwick
Co-Editors

ACCEPTED AND APPROVED FOR THE AUTHOR(S):

Author's signature:_____ Date: _____

___ All authors are U.S. Government officials or employees and prepared the submitted article as part of their official duties.